HHS Public Access

Author manuscript

J Pathol. Author manuscript; available in PMC 2023 February 01.

Published in final edited form as:

J Pathol. 2022 February ; 256(2): 223–234. doi:10.1002/path.5830.

BCG invokes superior STING-mediated innate immune response over radiotherapy in a carcinogen murine model of urothelial cancer

Kara A Lombardo[1,4,*], **Aleksandar Obradovic**[8,9,†], **Alok Kumar Singh**[5,†], **James L Liu**[1], **Gregory Joice**[1], **Max Kates**[1], **William Bishai**[5], **David McConkey**[4], **Alcides Chaux**[10], **Marie-Lisa Eich**[12], **M Katayoon Rezaei**[11], **George J Netto**[12], **Charles G Drake**[6,7,9], **Phuoc Tran**[1,3], **Andres Matoso**[1,2,4], **Trinity J Bivalacqua**[1,4,*]

[1]Department of Urology, The Johns Hopkins Medical Institutions, Baltimore, MD, USA.

[2]Department of Pathology, The Johns Hopkins Medical Institutions, Baltimore, MD, USA.

[3]Department of Radiation Oncology, The Johns Hopkins Medical Institutions, Baltimore, MD, USA.

[4]Greenberg Bladder Cancer Institute, The Johns Hopkins Medical Institutions, Baltimore, MD, USA

[5]Center for Tuberculosis Research, The Johns Hopkins Medical Institutions, Baltimore, MD, USA.

[6]Division of Urology, Oncology, Herbert Irving Comprehensive Cancer Center, Columbia University Medical Center, New York, NY, USA.

[7]Division Hematology and Oncology, Herbert Irving Comprehensive Cancer Center, Columbia University Medical Center, New York, NY, USA.

[8]Department of Systems Biology, Columbia University Irving Medical Center, New York, NY, USA.

[9]Center for Translational Immunology, Columbia University Irving Medical Center, New York, NY, USA.

[10]Department of Scientific Research, School of Postgraduate Studies, Norte University, 1614 Asunción, Paraguay.

[11]Department of Pathology, George Washington University, Washington, DC, USA.

[12]Department of Pathology, The University of Alabama at Birmingham, Birmingham, AL, USA.

[*]Correspondence to: KA Lombardo or TJ Bivalacqua, The Johns Hopkins Hospital, Marburg Building, Rm 405, 600 N Wolfe Street, Baltimore, MD 21287, USA. klombardo@jhmi.edu or tbivala1@jhmi.edu.

[†]These authors contributed equally

Author contributions statement

KAL designed the study, performed all experiments, collected samples, performed analysis, and wrote the manuscript. AO assisted with data analysis and edited the manuscript. AKS, JLL, GJ and MK assisted with experimental procedures and critical revision of the manuscript. CGD assisted with experimental design, data analysis and critical manuscript revision. PT assisted study design, experimental procedures, and critical manuscript revision. AM assisted with pathologic analysis and critical revision of manuscript. AC assisted with data analysis of human data and edited the manuscript. MLE and MKR assisted with human TMA pathologic and clinical data acquisition and edited the manuscript. GJN, DJM and WB assisted with data analysis and critical revision of the manuscript. TJB designed the research study, performed experimental oversight, and provided critical manuscript revision.

No conflicts of interest were declared

Abstract

Radiation and Bacillus Calmette-Guérin (BCG) instillations are used clinically for treatment of urothelial carcinoma, but the precise mechanisms by which they activate an immune response remain elusive. The role of the cGAS-STING pathway has been implicated in both BCG and radiation-induced immune response however comparison of STING-pathway molecules and immune landscape following treatment in urothelial carcinoma has not be performed. We therefore comprehensively analyzed the local immune response in the bladder tumor microenvironment following radiotherapy and BCG instillations in a well-established spontaneous murine model of urothelial carcinoma to provide insight into activation of STING-mediated immune response. Mice were exposed to the oral carcinogen, BBN, for 12 weeks prior to treatment with a single 15Gy dose of radiation or 3 intravesical instillations of BCG (1×10^8 CFU). At sacrifice, tumors were staged by a urologic pathologist and effects of therapy on the immune microenvironment were measured using the NanoString Myeloid Innate Immunity Panel and immunohistochemistry. Clinical relevance was established by measuring immune biomarker expression of cGAS and STING on a human tissue microarray consisting of BCG-treated non-muscle invasive urothelial carcinomas. BCG instillations in the murine model elevated STING and downstream STING-induced interferon and pro-inflammatory molecules, intratumoral M1 macrophage and T-cell accumulation, and complete tumor eradication. In contrast, radiotherapy caused no changes in STING pathway or innate immune gene expression; rather, it induced M2 macrophage accumulation and elevated FoxP3 expression characteristic of immunosuppression. In human non-muscle invasive bladder cancer, STING protein expression was elevated at baseline in patients who responded to BCG therapy and increased further after BCG therapy. Overall, these results show that STING pathway activation plays a key role in effective BCG-induced immune response and strongly indicate that the effects of BCG on the bladder cancer immune microenvironment are more beneficial than those induced by radiation.

Keywords

bladder cancer; innate immunity; tumor immune microenvironment; STING; BCG; radiotherapy; macrophages; T-cells; interferon; Trex-1

INTRODUCTION

One of the hallmarks of cancer is the generation of an immunosuppressive and tolerogenic tumor microenvironment (TME) consisting of malignant cells and immunosuppressive immune cell types such as tumor-associated macrophages, myeloid-derived suppressor cells, and regulatory T-cells (Tregs)[1–4]. The central goal of cancer immunotherapy is the recruitment of effector immune cells to the TME and restoration of competent immune activation to achieve optimal anti-tumor responses [4,5]. Intravesical Bacillus Calmette-Guérin (BCG) immunotherapy for non-muscle invasive bladder cancer (NMIBC) in immunocompetent individuals induces a robust antitumor immune response by engaging both the innate and adaptive arms of host immunity and is characterized by local infiltration of monocytes, inflammatory macrophages, neutrophils, natural killers and T-effector (Teff) cells [6–10]. As a key regulator of the type I interferon responses, the DNA sensing cGAS-stimulator of interferon genes (STING) pathway may contribute to the dynamic

reprogramming of innate immune cells in the bladder TME following BCG therapy [11]. STING activation and downstream effects cause a shift from an immunosuppressive to an immunostimulatory environment with significant representation of T-helper type-1 (Th1) pro-inflammatory cytokines, M1 macrophage polarization, and infiltration of Teff cells into the TME [7,11,12].

Radiotherapy (RT) has immunomodulatory effects in muscle invasive bladder cancer (MIBC)[13]. DNA-damage induced tumor-cell death following RT leads to accumulation of nucleic acids taken up by antigen presenting cells of the innate immune system resulting in activation of dendritic cells (DCs) and expression of STING-dependent type-I interferons and inflammatory cytokines [14,15]. However, radiation-induced genotoxic changes may elevate expression of exonucleases such as Trex-1 which degrade double-stranded cytoplasmic DNA (dsDNA) and may in turn diminish cGAS-STING-mediated interferon responses [16]. Despite studies showing that RT elicits some degree of immunostimulatory response, RT can also induce immunosuppressive Tregs and immune checkpoint molecules such as PD-L1 and CTLA-4 that effectively inhibit anti-tumor $CD8^+$ T-cell responses [17–19]. As such, several ongoing trials utilizing RT in combination with immunotherapy are now underway for both MIBC and NMIBC (SWOG/NRG-1806, ADAPT-BLADDER, PREVERT) [20–22].

Although studies have shown that baseline immunophenotype may predict response to RT in MIBC, data on changes in immune cell infiltrates in the bladder TME following RT for NMIBC are severely lacking [18,23]. Since Teff lymphocytes and macrophages are the main immune effectors in both RT and BCG immunotherapy, their immunophenotypic characterization in the bladder TME is essential for providing insight into the mechanisms by which these treatments invoke robust antitumor immunity and is crucial for development of novel therapeutic strategies for NMIBC. We hypothesized herein that RT would induce a differential local immune response in the bladder TME compared to BCG instillations and aimed to comprehensively analyze immune cell complexity and activation of STING-mediated inflammatory response utilizing the N-butyl-N-(4-hydroxybutyl)-nitrosamine (BBN) carcinogen murine model of urothelial cancer as well as characterize STING expression in human NMIBC pre- and post-BCG treatment.

MATERIALS AND METHODS

Ethics

All protocols involving animals strictly adhered to U.S. NIH guidelines and were approved by the Johns Hopkins Medical Institutions Animal Care and Use Committee under protocol M017M334.

BBN tumor model and treatments

Twenty-eight C57BL/6J female mice, 4–6 weeks of age (Jackson Laboratories, Bar Harbor, ME, USA) were separated into control (n=15) and BBN-induced tumor (n=13) groups with the latter receiving a continuous dose of 0.05% N-Butyl-N-(4-hydroxybutyl) nitrosamine (BBN) (cat# B0938; TCI Chemicals, Tokyo, Japan) in the drinking water. BBN exposure

was maintained for 12 weeks resulting in the development of carcinoma *in situ* (CIS) and treatment was initiated at week 12 to characterize effect on the bladder TME in mice with NMIBC [24]. Age-matched control and BBN-exposed animals were further randomized into three cohorts- untreated (n=9), RT (a single 15 Gy dose of external beam radiation) (n=10), or BCG (OncoTice®, Merck, Kenliworth, NJ, USA) (3 intravesical instillations, 100 μl at 1×10^8 CFU) (n=9) (supplementary material, Figure S1). Comparison of one dose of 15 Gy radiation versus 3 weekly intravesical BCG instillations at 1×10^8 CFU was based on previous studies where similarly administered therapies elicited a measurable immune response in rodent models [25,26]. To directly compare the effect of each therapy as a one-time treatment rather than at each respective immune response-eliciting dose, an additional group of BBN exposed mice (n=4) were treated at week 12 with one single instillation of BCG (TICE, 100 μl at 1×10^8 CFU). All animals were euthanized 3 days following their last treatment and bladders were harvested for analysis.

Histology and immunohistochemistry

Formalin-fixed paraffin embedded bladder sections were stained with hematoxylin and eosin (H&E) for tumor classification according to the World Health Organization/International Society of Urological Pathology consensus [27]. Tumor staging and disease involvement was performed by a board-certified genitourinary pathologist (A.M.). For all IHC staining, high-temperature antigen retrieval was performed in Tris/EDTA buffer, pH 9 (Agilent Technologies, Santa Clara, CA, USA) and manufacturers recommendations followed using Polyview Plus HRP-DAB detection kit (ENZO Life Sciences, Ann Arbor, MI, USA). Primary antibodies included Ki67 (clone SP6, dilution 1:50; cat# ab16667; Abcam, Cambridge, UK), CD4 (clone EPR19514, dilution 1:100, cat# ab183685; Abcam), CD8 (clone 53–6.7, dilution 1:50, cat# 550281; BD Pharmingen, San Diego, CA, USA), FoxP3 (clone D6O8R, dilution 1:50, cat# 12653S; Cell Signaling Technology, Danvers, MA, USA), STING (clone D2P2F, dilution 1:100, cat# 13647S; Cell Signaling Technology), Trex-1 (polyclonal, dilution 1:100, cat# ab83890, Abcam), CD86 (polyclonal, dilution 1:100, cat# GTX32507, GeneTex, Irvine, CA, USA) and CD206 (polyclonal, dilution 1:200, cat# NBP1–90020, Novus Biologicals, Littleton, CO, USA). All IHC stains were scored by a genitourinary pathologist blinded to BBN status or treatment group. Positively stained cells were counted in 10 random 40x high power fields (HPFs) and averaged for each marker. For Ki67, average nuclear positive cells were converted to percentage of positive cells per total cells in each HPF. Ki67-positivity was assessed separately in areas of urothelial cancer to evaluate tumor cell proliferation as well as in benign tissue to characterize proliferating immune cells in the stroma or urothelium [28].

NanoString analysis

Flash-frozen bladder tissue was processed for total RNA isolation using Qiagen RNeasy PowerLyzer Tissue & Cells Kits (cat# 15055–50; Qiagen, Hilden, Germany) and nCounter® Mouse Myeloid Innate Immunity Panel v2.0 (NanoString, Seattle, WA, USA) was used to analyze the mRNA expression from 12 control samples (4 untreated, 3 RT, 5 BCG) and 11 BBN samples (4 untreated, 4 RT, 3 BCG). NanoString count data were normalized to correct for background noise and differences in total gene count across samples. NanoString counts

for all genes were scaled to log2 (counts) and p-values and log-fold changes per gene were compared in each model and treatment group to quantify differentially expressed genes.

Human NMIBC tissue microarray

The use of human specimens was approved by the George Washington University Institutional Review Board and was deemed exempt from informed consent. To correlate STING activity seen in our BBN murine bladders with human data, TMAs constructed from 143 transurethral resection of bladder tumor (TURBT) specimens from 61 patients treated at George Washington University were stained for cGAS and STING expression. In every patient, the initial TURBT specimen at time of *de novo* diagnosis and all available subsequent TURBT samples during follow-up were included. Construction, clinical and pathological characteristics of the TMA have been previously reported [29]. Primary antibodies to STING (clone D2P2F, dilution 1:100, cat# 13647S, Cell Signaling Technology) and cGAS (clone D-9, dilution 1:1000, cat# sc-515777; Santa Cruz Biotech, Dallas, TX, USA) were used and slides were stained on a Ventana Ultra autostainer (Roche Diagnostics, Basel, Switzerland) using the UltraView DAB detection kit (cat# 760–500; Roche Diagnostics). The average percentage value of each marker was scored separately in tumor cells and immune cells across TMA cores in a given case was assigned as the expression score and used for further analysis.

In vitro infection assays and RT-qPCR analyses

The effects of BCG-mediated response in immune cells deficient in endogenous functional STING pathways was carried out in primary murine macrophages. In brief, bone marrow-derived macrophages (BMDMs) were generated from wild-type C57BL/6 (4 weeks of age, Charles River Laboratories, Willmington, MA, USA) and STING KO mice (C57BL/6J-Tmem173gt/J, Jackson Laboratories) as described previously[30]. Macrophages were infected at a ratio of 1:10 (macrophage versus BCG) for 24 h. Gene expression profiling of selected genes were carried out on RNA isolated using RNeasy Mini Kit (cat# 74004; Qiagen) to ascertain the effect of intact STING signaling following infection. TaqMan gene expression assays for *Cd86*, *Nos2*, *Cxcl10*, *Cd206*, *Il10*, *Cd274* and *Gapdh* were purchased (Applied Biosystem) and performed as described previously [31]. *Gapdh* was unchanged and served as an endogenous control.

Statistical analyses

Statistical analyses for murine data were performed in RStudio version 3.6.1 (RStudio, Boston, MA, USA). For each pairwise comparison of gene expression across treatment groups, we performed Benjamini–Hochberg multiple-testing correction and reported the number of differentially upregulated and downregulated genes with a corrected p-value < 0.05. Statistical significance of differential staining for IHC across treatment groups was assessed by pairwise Wilcox rank-sum test, with Benjamini–Hochberg multiple-testing correction. GraphPad Prism version 9.1.0 (GraphPad Inc, San Diego, CA, USA) was used for statistical human TMA data analyses and RT-qPCR profiling following murine in-vitro infection assay and significance of staining in sample groups was assessed by pairwise Wilcox rank-sum test.

RESULTS

BCG increases local immune cell infiltration to benign murine bladders

Histologic review of control murine bladders revealed benign urothelium with lymphocytic aggregates in the lamina propria seen in 3 of 5 (60%) bladders following BCG instillations that were not present in untreated or RT control bladders. (Figure 1A). Elevation of Ki67 expression in stromal immune cells and basal layer urothelial cells was seen following BCG instillations with average labeling of 10% compared to 1% in both untreated (p=0.03) and RT (p=0.03) groups (Figure 1A,B). Phenotypic assessment of lymphocytic infiltration revealed higher abundance of $CD4^+$ (11+ cells/HPF; p=0.02) and $CD8^+$ T-cells (5+ cells/HPF; p=0.03) following BCG instillations compared to untreated and RT bladders which had an average of <1+ cell/HPF each (Figure 1A,C,D).

BCG invokes a more robust antitumor immune response than radiotherapy

Histologic analyses revealed the highest pathologic tumor stage in untreated tumors to be CIS in all animals (100%). In tumor-bearing mice following a single dose of RT (15 Gy), 1 out of 5 (20%) mice was found to have MIBC, 3 out of 5 (60%) had CIS only, and 1 out of 5 (20%) showed a benign urothelial papilloma (Figure 2A,B). BBN-exposed bladders following 3 weekly instillations of BCG revealed a potent antitumor response with no evidence of CIS or invasive cancer, showing only benign urothelium with acute and chronic inflammation in all animals (Figure 2A,B). While the goal of this study was to compare the immune landscape following treatment rather than compare efficacy, it is notable that repeated intravesical instillations of BCG completely eradicated evidence of tumor, while animals receiving RT had a similar tumor involvement score as untreated tumors (29% vs 26%, respectively) (Figure 2C). IHC analyses of Ki67 expression were carried out to quantify proliferation in malignant cells as well as benign proliferating immune cells which revealed similar tumor proliferation indices in RT and untreated tumor groups (18% versus 26%, p=0.4) (Figure 2D,E). Ki67 evaluation in immune cells highlighted the inflammation seen on H&E following BCG therapy with 70% expression in benign inflammatory cells in the stroma and urothelium compared to 9% in RT (p=0.03) and 8% in untreated (p=0.04) (Figure 2F). Histologic review of murine bladders exposed to one single dose of BCG revealed residual CIS in 3 of 4 murine bladders (75%) while the remaining bladder showed benign denuded urothelium with all bladders exhibiting inflammation in the lamina propria on H+E (supplementary material, Figure S2A).

NanoString data revealed BBN activated innate immune cells, such that samples exposed to BBN were strongly separated in a 2-dimensional UMAP projection of global gene expression, and innate immunity genes were more highly expressed in BBN-exposed samples in a hierarchically clustered gene expression heatmap (Figure 3A,B). Genes plotted by log fold-change (logFC) and statistical significance revealed significant differential expression of genes in BBN-exposed samples compared to controls (Figure 3C–E). Gene ontology analysis of upregulated genes by >2 logFC in untreated BBN tumors revealed 24 upregulated innate immunity genes, including immunosuppressive genes (*Ccl22*, *Il33*, *Il1rn*, *Areg*, *Ctla4*, *Ccl8*), pro-inflammatory genes (*Isg15*, *Cxcl9*, *Cxcl10*, *Irf7*, *Il18*), genes involved in T-cell trafficking (*Ccr7*, *Ccl5*, *Sell*, *Ccl12*, *C4a*, *Ltb*, *Itgal*, *Ptprc*) and neutrophil

activation (*Adam8*, *Fcgr4*). A full list of genes differentially expressed by >2 logFC in BBN groups compared to control bladders may be found in supplementary material, Table S1.

Gene expression analyses comparing treatment groups among BBN-exposed samples revealed no significant changes in innate immune cell activation following RT (Figure 3F). Conversely, intravesical BCG instillations led to robust innate immune cell activation in the TME visualized by distance between gene clusters in heat map and UMAP analyses (Figure 3A,B). Associated volcano plots show significant differential expression of 473 individual genes following BCG instillations compared to untreated (Figure 3G) and 375 compared RT (Figure 3H). Evaluation of genes upregulated by >2 logFC following BCG instillations revealed genes involved in chemotactic activity that assist in lymphoid and myeloid trafficking (*Chil3*, *Frp2*, *Cxcl10* and *Ccl2*), pro-inflammatory markers (*Il1b*, *Nos2*, *Tmem173*), and T-cell homing (*Sell*). Interestingly, several genes involved in immunosuppression and immune checkpoints (*Arg1*, *Ido1*, *Cd274*, *Clec5a* and *Cd38a*) and assist in recruitment of immunosuppressive myeloid cells (*S100a8* and *S100a9*) were also elevated in response to BCG underscoring the complexity of BCG-induced immune response. A full list of genes upregulated following BCG instillations may be found in supplementary material, Table S2.

BCG-induced antitumor response is characterized by increased STING expression and downstream pro-inflammatory effects as compared to radiotherapy

As RT and BCG are known to impact the inflammatory immune response, we compared their effects on inducing key inflammatory markers that are known to be upregulated in NMIBC as well as markers that have been shown to correlate with BCG or RT. Significant upregulation of known markers associated with positive response to BCG therapy including pro-inflammatory cytokines *Il2* (p=0.04), *Il6* (p=0.003), Il12a, (p=0.009), *Csf2* (p=0.04), *Ifng* (p=0.006), *Tnfa* (p=0.003), *Il1b* (p=0.003), chemokine *Cxcl10* (p=0.003), transcription factor *Stat1* (p=0.002) and isoenzyme *Nos2* (p=0.0002) was observed following BCG instillations, whereas RT did not induce expression of any of these molecules (Figure 4A). Next, we evaluated immunosuppressive molecules associated with higher disease stage and progression of NMIBC (*Tgfb*, *Il10*, *Il4*, *Il9*, *Il13*, *Stat3*, *Ido1*) and immune check point genes *Ctla4* and *Cd274* (PD-L1). Interestingly, none of these markers were upregulated in RT or untreated tumor groups, while several were elevated following BCG instillations despite lack of residual tumor, including cytokines *Il10* (p=0.03) and *Tgfb1* (p=0.0006) as well as *Ido1* (p=0.001) and checkpoint molecules *Ctla4* (p=0.03) and *Cd274* (p=0.0005) (Figure 4B). Since Th1/Th2 cytokine expression ratios correlate with monocyte differentiation to either classically activated immunostimulatory macrophages or alternatively activated immunosuppressive macrophages, respectively, we next queried macrophage polarization phenotypes using mRNA and protein levels of *Cd86* (M1 maker) and *Cd206* (M2 marker). Despite elevation of certain Th2 cytokines following BCG therapy, the abundant expression of key Th1 cytokines resulted in an overall shift toward M1 macrophage polarization as evidenced by elevated *Cd86* mRNA (2.8 logFC, p=0.0006) as well as a 50% increase in CD86 protein expression (Figure 4C). In both RT and untreated tumor groups there was no difference in mRNA expression of *Cd86* or *Cd206* (Figure 4C,D), however CD206 protein expression by IHC in both these groups was elevated (Figure 4D).

To explore a potential functional link between the BCG-induced inflammatory response outlined above and STING signaling, we next quantified levels of STING itself, as well as exonuclease Trex-1, a key regulator of the cGAS-STING pathway. Following three BCG instillations, we observed significant elevation of *Tmem173* mRNA (average 2.5 logFC, p=0.0005), and average 90% increase in STING protein levels (p=0.02) in all mice (n=4) which was consistent with the robust inflammatory response seen in these samples (Figure 4E). In murine bladders treated with just one instillation of BCG, we similarly saw elevation of STING protein expression by IHC compared to untreated tumor (p=0.03) in all animals. (supplementary material, Figure S2A,B). In contrast, RT had no effect on STING mRNA (p = 0.9) or protein (p = 0.1) expression in any sample, consistent with the overall lack of immune response observed following RT (Figure 4E). While *Trex1* was not statistically elevated at the mRNA level (0.95 logFC, p=0.40), a single RT dose of 15Gy to the BBN bladder resulted in elevated protein expression as analyzed by IHC (25%, p=0.03) (Figure 4F). Interestingly, BCG instillations caused significant elevation of Trex-1 at both mRNA (p=0.001) and protein levels (p=0.03) (Figure 4F).

To assess the effect of STING-mediated immune activation on recruitment of infiltrating lymphocytes to the bladder following BCG and RT, we performed IHC for CD4, CD8 and FoxP3 (Figure 5A). Despite a lack of elevated immunosuppressive cytokines at the mRNA level, higher expression of FoxP3 protein was seen in untreated (20+cells/HPF, p=0.03) and RT (10+cells/HPF, p=0.02) bladders, while nearly absent following 3 BCG instillations (<1+cell/HPF). Additionally, RT and untreated tumor groups revealed low numbers of CD4+ and CD8+ positive cells, resulting in low Teff to Treg ratios, which have been shown to correlate with worsening disease, early recurrence, and progression of urothelial cancer in both preclinical and clinical settings [32,33]. Significantly elevated numbers of $CD4^+$ and $CD8^+$ cells seen in the bladder TME following three repeated BCG instillations highlights the effect of pro-inflammatory molecules in recruiting Teffs to the TME, resulting in an immune activated environment with a nearly 25% increase in $CD4^+/FoxP3^+$ (p=0.04) and $CD8^+/FoxP3^+$ (p=0.04) ratios (Figure 5B,C). Additionally, following just one BCG instillation we similarly saw an increase in both CD8+ (p=0.03) and CD4+ (p=0.057) T-cells compared to untreated tumor (supplementary material, Figure S2A,C,D). Consistent with previous work reported by our group, elevation of CD8+ T-cells was noted following BCG instillations shown by a trend toward increased CD8+/CD4+ ratio (p=0.1) (Figure 5D) [31].

BCG-induced inflammation response is reliant on intact STING signaling

The crucial role of the STING pathway in inducing inflammatory response following BCG therapy was confirmed by significantly reduced expression of inflammatory molecules on STING knockout (STING KO) BMDMs following infection with BCG including M1 macrophage markers *Cd86* and *Nos2* and chemokine *Cxcl10* (supplementary material, Figure S3A–C). In addition to pro-inflammatory molecules, we observed reduced expression of *Il10* and *Cd274* in these STING KO BMDMs following BCG, indicating the STING pathway may be responsible for inducing certain immunosuppressive genes as well (supplementary material, Figure S3D,E). Conversely, immunosuppressive macrophage marker *Cd206* was elevated in STING KO BMDMs following BCG infection and was

significantly reduced in wild type BMDMs after treatment with BCG (supplementary material, Figure S3F).

STING expression in human NMIBC predicts response to BCG therapy

To attempt to validate our observation that elevated STING pathway activation occurs following BCG therapy, we performed IHC for cGAS and STING on human NMIBC. Our TMA had scoring data available for 42 treatment naïve patient samples including 18 cases of LGTa, 6 cases of HGTa, and 18 cases of T1 (supplementary material, Table S3). Average STING expression in tumor cells decreased with higher grade and stage disease with average expression of 22% in LGTa, 15% in HGTa and 6.5% in T1($p=0.03$) (Figure 6A,B) while there was no change in expression in inflammatory cells (supplementary material, Figure S5). There was no difference in cGAS expression among tumor stage and grade, nor post-BCG or among BCG responders (supplementary material, Figure S4A–C). Nineteen patients in this TMA cohort received BCG therapy, of these, scoring data was available for both pre- and post-BCG samples of 14 patients who had a tumor recurrence following BCG. STING expression was significantly elevated in tumor cells post-BCG therapy, with average expression of 25% compared to 5.3% pre-treatment ($p=0.04$) (Figure 6D,E). In pre-BCG treated samples with available tissue for scoring, STING expression was higher at baseline in samples from patients who did not have a tumor recurrence at their next biopsy (16%) compared to those who did have tumor recurrence (2.3%) ($p=0.01$) (Figure 6D). STING expression in inflammatory cells remained highly expressed in pre- and post-BCG tissue and regardless of outcome relating to recurrence (supplementary material, Figure S5).

DISCUSSION

Using the BBN murine model of urothelial cancer, we compared the differential effects of two clinically-relevant immune modulators (RT and BCG) on the cellular composition of the bladder TME to provide insight into mechanistic differences in activation of STING-mediated immune response. Our results demonstrate that despite BCG inducing molecules involved in immunosuppressive pathways, an overwhelming upregulation of STING and STING-mediated pro-inflammatory Th1-type molecules resulted in an immunostimulatory environment with predominant M1 macrophage differentiation and induction of robust T-effector cell infiltration accompanied by complete tumor regression. These data, validated by in vitro STING KO studies in murine BMDMs as well as human NMIBC tumor cells suggest that activation of the STING pathway contributes to the innate antitumor effects of BCG. Conversely, RT used at the dose and fractionation scheme we employed here did not induce any significant localized anti-tumor immune response. Consistent with previous findings, we observed increased levels of the DNA exonuclease Trex-1 following RT, which may have inhibited the STING-dependent induction of innate immune response and could help explain why RT caused no significant inflammatory changes [16].

While the precise mechanism of BCG’s efficacy in management of NMIBC remains uncertain, the BCG-induced immune response accountable for antitumor activity has been well documented, with evidence supporting the roles of both innate and adaptive immunity[9,10,31,34,35]. Recent work has implicated the interferon inducing cGAS-STING

pathway as a mechanistic activator of BCG-induced immune response [11]. In patients receiving BCG immunotherapy, cytoplasmic dsDNA sensing by cGAS secondary to BCG-induced immunogenic cell death may activate STING through formation of cyclic GMP-AMP (cGAMP). However, BCG as a bacterial molecule also upregulates pathways that generate small molecule STING agonists such as c-di-AMP that mimic the effect of cGAMP and bind directly to STING receptors for activation[36,37]. As an adaptor protein that may be expressed in both tumor and immune cells, STING facilitates signaling complexes, including phosphorylation of Irf3, which activate transcription of type I interferons and interferon stimulated genes such as *Ifng*, *Cxcl10*, and *Il6* [38]. Furthermore, cGAS-STING activation within the TME leads to elevation of $CD11b^+$ DCs and macrophages resulting in the expression of innate cytokines *Csf2*, *Il2*, *Il1b* and *Tnfa* as well as macrophage polarization to M1 pro-inflammatory subtype, all of which are essential for recruitment of $CD8^+$ T-cells to the TME and have been shown to correlate with successful immune rejection of tumors following BCG therapy [39–43]. Our BBN murine bladders following BCG instillations exhibit these downstream effects of STING activation (pro-inflammatory chemokine and cytokine expression, M1 macrophage polarization and CD8+ T-cell recruitment) along with elevated STING expression itself in immune cells recruited to the bladder, implicating the STING pathway as a crucial mediator of this successful BCG-induced anti-tumor response.

Human NMIBC TMA data showing decreased STING expression in tumors with higher grade and stage suggest that the STING pathway may play a role in tumorigenesis. Decreased expression of STING among higher grade and stage was found to be consistent with reported findings of low or absent expression in more aggressive forms of colorectal and gastric cancers [44,45]. Furthermore, higher STING expression at baseline in tumors that responded favorably to BCG implicate the potential of STING signaling in mechanisms of BCG response and/or resistance. Despite low baseline STING expression among BCG non-responders, STING expression was elevated in tumor samples at time of recurrence following BCG therapy in paired samples from the same patients, highlighting changes in the phenotype of these tumors to express STING following BCG instillations. This expression may be induced by c-di-AMPs secreted from BCG molecules, or otherwise a result of changes in the tumor immune microenvironment secondary to BCG-induced immune cell recruitment. The underlying causes of this change in expression require further studies to assess the direct effect of BCG on activation of STING in tumor cells. BCG unresponsive tumors may be susceptible to novel combination therapies exploiting the STING signaling pathway. Such methods have already been proposed in clinical trials testing STING agonists as a salvage therapy in BCG non-responders (NCT04109092), as well as current studies by our group testing efficacy of a recombinant BCG-STING strain in rodent bladder cancer models [46,47].

Although BCG generates a predominantly pro-inflammatory response, it may also result in upregulation of immunosuppressive pathways such as the PD1/PD-L1 axis, as is the basis for current clinical trials investigating the use of immune checkpoint blockades following either unsuccessful or in combination with intravesical BCG instillations (ADAPT-BLADDER, KEYNOTE-057, POTOMAC)[6,7,48–50]. Our data supports the underlying rationale for these trials, as BCG instillations upregulated checkpoint molecules

Cd274 (PD-L1), *Pdcd1* (PD1) and *Ctla4* as well as *Ido1*, a key enzyme involved in tryptophan metabolism. The enzyme indoleamine 2, 3-dioxygenase (IDO1) has been shown to promote epithelial-mesenchymal transition in several cancers, including bladder, and as such the use of IDO1 inhibitors in combination with immune checkpoint inhibitor nivolumab have shown promising results in advanced stage cancers (NCT02658890) [51]. Significant elevation of *Ido1* following BCG instillations in this study indicate the potential for synergistic effects of combining clinically-available IDO1 inhibitors with BCG to enhance the durability of responses and potentially avoid BCG resistance. Despite elevation of Th2 cytokines such as *Tgfb* and *Il10* at an mRNA level following BCG instillation, there was no evidence of T-cell inhibition at the protein level and successful eradication of tumor highlights that the robust pro-inflammatory response induced by BCG here was sufficient to shift the TME toward an overall immunostimulatory environment.

Despite data showing both the immunostimulatory and immunosuppressive potential of RT in several types of cancer including MIBC, RT in our BBN murine model produced little effect on the local immune response in the bladder [52,53]. There was no significant elevation of neither pro- nor anti-inflammatory innate immunity genes following RT, including immune checkpoint molecules PD-L1 and CTLA4, which have been widely noted to be upregulated following RT in MIBC [23,54]. As typical immunosuppressive markers have been shown to correlate with progression of disease and higher stage of MIBC, it is possible that we did not observe an extensive immunosuppressive profile because the tumors in our study were mostly non-invasive. Similar to BCG therapy, the cGAS-STING pathway has been implicated in anti-tumor immunity following RT, activation of which caused by cytoplasmic dsDNA accumulation [14,15]. While STING expression was evident in immune and tumor cells in the BBN murine bladder TME following RT, levels were unchanged compared to untreated tumor as measured by NanoString and IHC, consistent with the lack of any robust inflammatory response observed in these samples. Previous *in vivo* and *in vitro* studies in breast cancer and colorectal carcinoma murine models and cell lines suggest that the DNA exonuclease, Trex-1, is a key regulator of the cGAS-STING pathway, and elevated doses of RT between 12–18 Gy induce excess pooled nucleic acid which elevate levels of Trex-1 such that detection by cGAS is evaded [16]. We did not observe increased *Trex1* mRNA expression, though IHC results suggest elevated Trex-1 protein expression, possibly explaining the lack of cGAS-STING-IRF3 axis activation. Interestingly, Trex-1 expression was also significantly induced by BCG at both mRNA and protein levels. However, while STING activation in response to RT is reliant on cytoplasmic dsDNA to activate cGAS and then STING, c-di-AMP secreted by BCG may bind directly to STING and bypass the need for cGAS to activate this pathway. The superior anti-tumor immunity observed by BCG instillations may be a direct consequence of the potential adjuvant benefits of such STING activating mechanisms as compared to RT, especially in the case of NMIBC.

Limitations of our study must be acknowledged, including small sample size in the BBN murine model as well as the fact that our NanoString analysis on mixed urothelial/immune cell tissue consisted of an innate immunity panel rather than whole transcriptome sequencing. Additionally, Trex-1 levels have been shown to remain unchanged following multiple fractionated doses of 8Gy radiation in vivo and in vitro, therefore, testing lower fractionated doses of RT is warranted as are mechanistic studies confirming the

effect of Trex-1 on STING inhibition in this setting [16]. Finally, human TMA findings demonstrating STING expression in these samples must be validated in a larger cohort including cases of CIS as well as whole slide sections to address tumor heterogeneity in NMIBC. The implications of the STING pathway as a mediator of BCG efficacy require further mechanistic studies to determine whether the observed STING activation in tumor and immune cells and downstream anti-tumor effects are a direct result of BCG.

In summary, we report an association between the recruitment of immune cells proficient in STING signaling to the bladder TME and the local robust pro-inflammatory response seen following BCG instillations in a BBN murine model of NMIBC. We further highlight high STING activity in human NMIBC both following BCG therapy and in patients who responded to BCG therapy. In addition to a pro-inflammatory response, BCG elicited expression of key T-cell inhibiting molecules that may be targeted to improve BCG's efficacy and may in part explain the lack of antitumor efficacy in BCG non-responders. RT in this model, given as a single dose of 15 Gy, had no significant anti-tumor effect in the bladder TME, though increased levels of Trex-1 may have inhibited the cGAS-STING-dependent induction of pro-inflammatory immune response. These findings provide insight into the local innate anti-tumor response mediated through cGAS-STING pathway activation induced by BCG but not RT in NMIBC and are essential for understanding how to enhance current therapeutic options and guide development of novel clinical trial designs for management of bladder cancer.

Supplementary Material

Refer to Web version on PubMed Central for supplementary material.

Acknowledgements

We gratefully acknowledge the support of NIH AI 155346.

Data availability statement

All Nanostring data is stored in a GEO database repository and can be found at https://www.ncbi.nlm.nih.gov/geo/query/acc.cgi?acc=GSE186737.

REFERENCES

1. Satyam A, Singh P, Badjatia N, et al. A disproportion of TH1/TH2 cytokines with predominance of TH2, in urothelial carcinoma of bladder. Urol Oncol 2011; 29: 58–65. [PubMed: 19837616]
2. Eruslanov E, Neuberger M, Daurkin I, et al. Circulating and tumor-infiltrating myeloid cell subsets in patients with bladder cancer. Int J Cancer 2012; 130: 1109–1119. [PubMed: 21480223]
3. Balkwill FR, Capasso M, Hagemann T. The tumor microenvironment at a glance. J Cell Sci 2012; 125: 5591–5596. [PubMed: 23420197]
4. Quail DF, Joyce JA. Microenvironmental regulation of tumor progression and metastasis. Nat Med 2013; 19: 1423–1437. [PubMed: 24202395]
5. Kershaw MH, Devaud C, John LB, et al. Enhancing immunotherapy using chemotherapy and radiation to modify the tumor microenvironment. Oncoimmunology 2013; 2: e25962. [PubMed: 24327938]

6. Watanabe E, Matsuyama H, Matsuda K, et al. Urinary interleukin-2 may predict clinical outcome of intravesical bacillus Calmette-Guerin immunotherapy for carcinoma in situ of the bladder. Cancer Immunol Immunother 2003; 52: 481–486. [PubMed: 12707736]
7. Pichler R, Fritz J, Zavadil C, et al. Tumor-infiltrating immune cell subpopulations influence the oncologic outcome after intravesical Bacillus Calmette-Guerin therapy in bladder cancer. Oncotarget 2016; 7: 39916–39930. [PubMed: 27221038]
8. Ratliff TL, Ritchey JK, Yuan JJ, et al. T-cell subsets required for intravesical BCG immunotherapy for bladder cancer. J Urol 1993; 150: 1018–1023. [PubMed: 8102183]
9. Brandau S, Riemensberger J, Jacobsen M, et al. NK cells are essential for effective BCG immunotherapy. Int J Cancer 2001; 92: 697–702. [PubMed: 11340575]
10. Suttmann H, Riemensberger J, Bentien G, et al. Neutrophil granulocytes are required for effective Bacillus Calmette-Guerin immunotherapy of bladder cancer and orchestrate local immune responses. Cancer Res 2006; 66: 8250–8257. [PubMed: 16912205]
11. Koti M, Chenard S, Nersesian S, et al. Investigating the STING Pathway to Explain Mechanisms of BCG Failures in Non-Muscle Invasive Bladder Cancer: Prognostic and Therapeutic Implications. Bladder Cancer 2019; 5: 225–234.
12. Ingersoll MA, Albert ML. From infection to immunotherapy: host immune responses to bacteria at the bladder mucosa. Mucosal Immunol 2013; 6: 1041–1053. [PubMed: 24064671]
13. Daro-Faye M, Kassouf W, Souhami L, et al. Combined radiotherapy and immunotherapy in urothelial bladder cancer: harnessing the full potential of the anti-tumor immune response. World Journal of Urology 2020: 1–13. [PubMed: 31788716]
14. Burnette BC, Liang H, Lee Y, et al. The efficacy of radiotherapy relies upon induction of type I interferon–dependent innate and adaptive immunity. Cancer research 2011; 71: 2488–2496. [PubMed: 21300764]
15. Zhang F, Manna S, Pop LM, et al. Type I Interferon Response in Radiation-Induced Anti-Tumor Immunity. In: Seminars in Radiation Oncology. (ed)^(eds). Elsevier, 2020; 129–138.
16. Vanpouille-Box C, Alard A, Aryankalayil MJ, et al. DNA exonuclease Trex1 regulates radiotherapy-induced tumour immunogenicity. Nature communications 2017; 8: 15618.
17. Liu S, Sun X, Luo J, et al. Effects of radiation on T regulatory cells in normal states and cancer: mechanisms and clinical implications. American journal of cancer research 2015; 5: 3276. [PubMed: 26807310]
18. Wu C-T, Chen W-C, Chang Y-H, et al. The role of PD-L1 in the radiation response and clinical outcome for bladder cancer. Scientific reports 2016; 6: 19740. [PubMed: 26804478]
19. Muroyama Y, Nirschl TR, Kochel CM, et al. Stereotactic radiotherapy increases functionally suppressive regulatory T cells in the tumor microenvironment. Cancer immunology research 2017; 5: 992–1004. [PubMed: 28970196]
20. Chemoradiotherapy With or Without Atezolizumab in Treating Patients With Localized Muscle Invasive Bladder Cancer [Accessed 28 October 21: Available from: https://clinicaltrials.gov/ct2/show/NCT03775265
21. ADAPT-BLADDER: Modern Immunotherapy in BCG-Relapsing Urothelial Carcinoma of the Bladder [Accessed 28 October 21: Available from: https://clinicaltrials.gov/ct2/show/NCT03317158
22. Bladder PREserVation by RadioTherapy and Immunotherapy in BCG Unresponsive Non-muscle Invasive Bladder Cancer (PREVERT) [Accessed 28 October 2021: Available from: https://clinicaltrials.gov/ct2/show/NCT03950362
23. Gong J, Le TQ, Massarelli E, et al. Radiation therapy and PD-1/PD-L1 blockade: the clinical development of an evolving anticancer combination. Journal for immunotherapy of cancer 2018; 6: 46. [PubMed: 29866197]
24. Oliveira PA, Vasconcelos-Nobrega C, Gil da Costa RM, et al. The N-butyl-N-4-hydroxybutyl Nitrosamine Mouse Urinary Bladder Cancer Model. Methods Mol Biol 2018; 1655: 155–167. [PubMed: 28889385]
25. Wada S, Harris TJ, Tryggestad E, et al. Combined treatment effects of radiation and immunotherapy: studies in an autochthonous prostate cancer model. International Journal of Radiation Oncology* Biology* Physics 2013; 87: 769–776.

26. Huang P, Ma C, Xu P, et al. Efficacy of intravesical Bacillus Calmette-Guérin therapy against tumor immune escape in an orthotopic model of bladder cancer. Experimental and therapeutic medicine 2015; 9: 162–166. [PubMed: 25452795]
27. Comperat EM, Burger M, Gontero P, et al. Grading of Urothelial Carcinoma and The New "World Health Organisation Classification of Tumours of the Urinary System and Male Genital Organs 2016". Eur Urol Focus 2019; 5: 457–466. [PubMed: 29366854]
28. Wang C, Ross WT, Mysorekar IU. Urothelial generation and regeneration in development, injury, and cancer. Developmental Dynamics 2017; 246: 336–343. [PubMed: 28109014]
29. Eich ML, Chaux A, Guner G, et al. Tumor immune microenvironment in non-muscle-invasive urothelial carcinoma of the bladder. Hum Pathol 2019; 89: 24–32. [PubMed: 31026471]
30. Marim FM, Silveira TN, Lima DS Jr., et al. A method for generation of bone marrow-derived macrophages from cryopreserved mouse bone marrow cells. PLoS One 2010; 5: e15263. [PubMed: 21179419]
31. Kates M, Nirschl T, Sopko NA, et al. Intravesical BCG induces CD4+ T-cell expansion in an immune competent model of bladder cancer. Cancer immunology research 2017; 5: 594–603. [PubMed: 28588015]
32. Baras AS, Drake C, Liu J-J, et al. The ratio of CD8 to Treg tumor-infiltrating lymphocytes is associated with response to cisplatin-based neoadjuvant chemotherapy in patients with muscle invasive urothelial carcinoma of the bladder. Oncoimmunology 2016; 5: e1134412. [PubMed: 27467953]
33. Parodi A, Traverso P, Kalli F, et al. Residual tumor micro-foci and overwhelming regulatory T lymphocyte infiltration are the causes of bladder cancer recurrence. Oncotarget 2016; 7: 6424. [PubMed: 26824503]
34. Higuchi T, Shimizu M, Owaki A, et al. A possible mechanism of intravesical BCG therapy for human bladder carcinoma: involvement of innate effector cells for the inhibition of tumor growth. Cancer immunology, immunotherapy 2009; 58: 1245–1255. [PubMed: 19139883]
35. Kleinnijenhuis J, Quintin J, Preijers F, et al. Long-lasting effects of BCG vaccination on both heterologous Th1/Th17 responses and innate trained immunity. Journal of innate immunity 2014; 6: 152–158. [PubMed: 24192057]
36. Dey B, Dey RJ, Cheung LS, et al. A bacterial cyclic dinucleotide activates the cytosolic surveillance pathway and mediates innate resistance to tuberculosis. Nat Med 2015; 21: 401–406. [PubMed: 25730264]
37. Dey RJ, Dey B, Singh AK, et al. Bacillus Calmette-Guerin Overexpressing an Endogenous Stimulator of Interferon Genes Agonist Provides Enhanced Protection Against Pulmonary Tuberculosis. J Infect Dis 2020; 221: 1048–1056. [PubMed: 30901058]
38. Woo S-R, Fuertes MB, Corrales L, et al. STING-dependent cytosolic DNA sensing mediates innate immune recognition of immunogenic tumors. Immunity 2014; 41: 830–842. [PubMed: 25517615]
39. Da Hoong BY, Gan YH, Liu H, et al. cGAS-STING pathway in oncogenesis and cancer therapeutics. Oncotarget 2020; 11: 2930. [PubMed: 32774773]
40. Klarquist J, Hennies CM, Lehn MA, et al. STING-mediated DNA sensing promotes antitumor and autoimmune responses to dying cells. The Journal of Immunology 2014; 193: 6124–6134. [PubMed: 25385820]
41. Francica BJ, Ghasemzadeh A, Desbien AL, et al. TNFα and radioresistant stromal cells are essential for therapeutic efficacy of cyclic dinucleotide STING agonists in nonimmunogenic tumors. Cancer immunology research 2018; 6: 422–433. [PubMed: 29472271]
42. Ohkuri T, Kosaka A, Ishibashi K, et al. Intratumoral administration of cGAMP transiently accumulates potent macrophages for anti-tumor immunity at a mouse tumor site. Cancer Immunology, Immunotherapy 2017; 66: 705–716. [PubMed: 28243692]
43. Corrales L, Glickman LH, McWhirter SM, et al. Direct activation of STING in the tumor microenvironment leads to potent and systemic tumor regression and immunity. Cell reports 2015; 11: 1018–1030. [PubMed: 25959818]
44. Xia T, Konno H, Ahn J, et al. Deregulation of STING Signaling in Colorectal Carcinoma Constrains DNA Damage Responses and Correlates With Tumorigenesis. Cell Rep 2016; 14: 282–297. [PubMed: 26748708]

45. Song S, Peng P, Tang Z, et al. Decreased expression of STING predicts poor prognosis in patients with gastric cancer. Sci Rep 2017; 7: 39858. [PubMed: 28176788]

46. A Study of Stimulator of Interferon Genes (STING) Agonist E7766 in Non-muscle Invasive Bladder Cancer (NMIBC) Including Participants Unresponsive to Bacillus Calmette-Guerin (BCG) Therapy, INPUT-102 [Accessed 28 October 21: Available from: https://clinicaltrials.gov/ct2/show/NCT04109092

47. Singh AK, Praharaj M, Lombardo KA, et al. Recombinant BCG overexpressing a STING agonist elicits trained immunity and improved antitumor efficacy in non-muscle invasive bladder. bioRxiv 2020 [Not peer reviewed].

48. Redelman-Sidi G, Glickman MS, Bochner BH. The mechanism of action of BCG therapy for bladder cancer—a current perspective. Nature Reviews Urology 2014; 11: 153. [PubMed: 24492433]

49. Chevalier MF, Schneider AK, Cesson V, et al. Conventional and PD-L1-expressing regulatory T cells are enriched during BCG therapy and may limit its efficacy. European urology 2018; 74: 540–544. [PubMed: 30033046]

50. Kates M, Matoso A, Choi W, et al. Adaptive immune resistance to intravesical BCG in non–muscle invasive bladder cancer: Implications for prospective BCG-unresponsive trials. Clinical Cancer Research 2020; 26: 882–891. [PubMed: 31712383]

51. Zhang W, Zhang J, Zhang Z, et al. Overexpression of indoleamine 2, 3-dioxygenase 1 promotes epithelial-mesenchymal transition by activation of the IL-6/STAT3/PD-L1 pathway in bladder cancer. Translational oncology 2019; 12: 485–492. [PubMed: 30594037]

52. Thompson RF, Maity A. Radiotherapy and the tumor microenvironment: mutual influence and clinical implications. In: Tumor Microenvironment and Cellular Stress. (ed)^(eds). Springer, 2014; 147–165.

53. Grassberger C, Ellsworth SG, Wilks MQ, et al. Assessing the interactions between radiotherapy and antitumour immunity. Nature Reviews Clinical Oncology 2019: 1–17.

54. Dovedi SJ, Adlard AL, Lipowska-Bhalla G, et al. Acquired resistance to fractionated radiotherapy can be overcome by concurrent PD-L1 blockade. Cancer research 2014; 74: 5458–5468. [PubMed: 25274032]

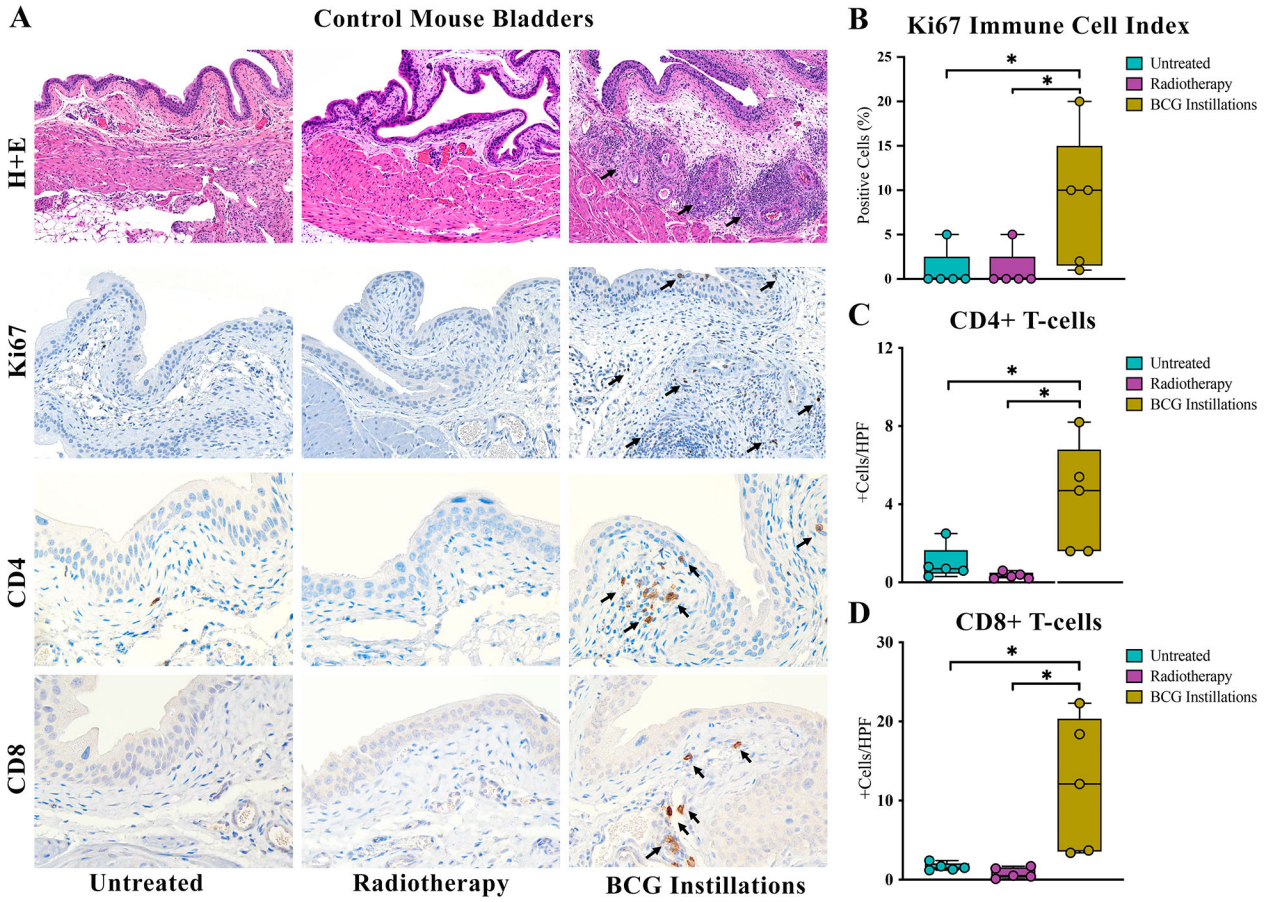

Figure 1. BCG elicited infiltration of immune cells to control mouse bladders.

Histologic examination revealed lymphocytic infiltrates in 60% of benign murine bladders following BCG not seen in other treatment groups (**A, top row, arrows**). Proliferating immune cells marked by nuclear Ki67 expression and $CD4^+$ and $CD8^+$ T-cells were significantly elevated following BCG instillations (**A, arrows, B, C, D**). * $p < 0.05$. Calibration bar 100μm.

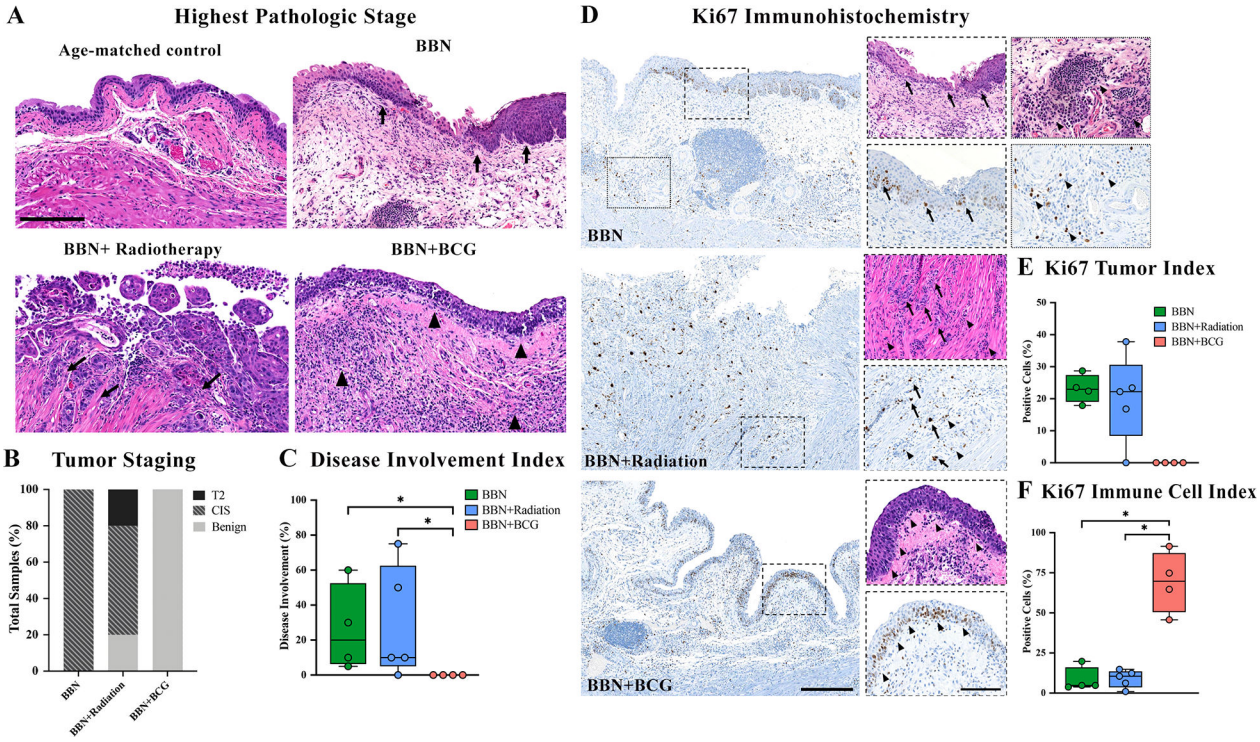

Figure 2. BCG elicits superior anti-tumor immune response compared to radiotherapy.

Representative histologic images show untreated BBN-induced carcinoma *in situ* (**A, arrows, calibration bar 100μm**), muscle invasive urothelial carcinoma following radiotherapy (**A, arrow**), and benign urothelium with acute and chronic inflammation (**A, arrows**) following BCG instillations along with tumor staging for all samples (**B**). Disease involvement index highlights efficacy of BCG instillations on reduction of tumor as compared to radiotherapy (**C**). Ki67 nuclear expression in BBN-exposed samples (**calibration bar 50μm**) with inset (**calibration bar 100μm)** showing positive expression in tumor cells (**D, arrows**) and benign immune cells (**D, stars**). Inverse Ki67 tumor index (**E**) and immune cell index (**F**) highlights role of immune cell infiltration in eradication of tumor. ***** $p < 0.05$.

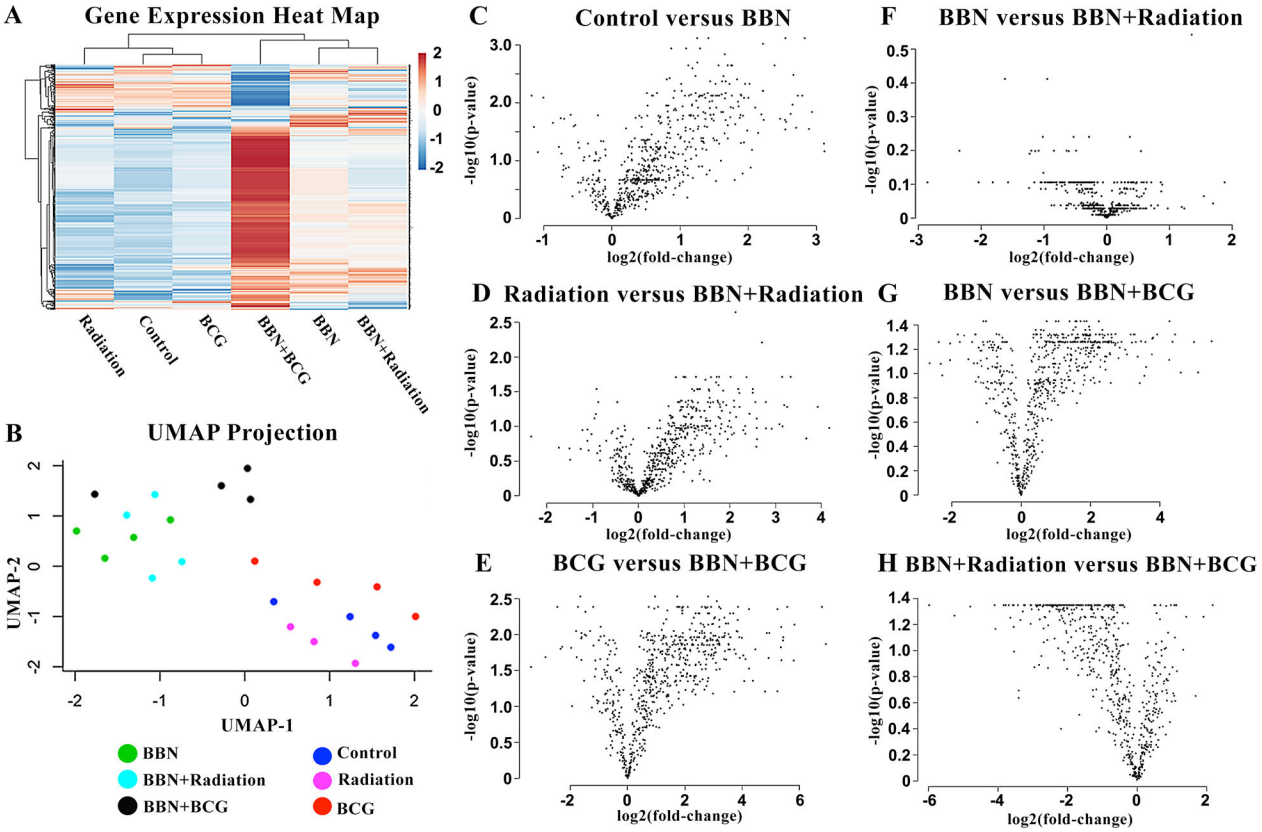

Figure 3. NanoString analyses of innate immunity genes reveals activation by BBN carcinogen and BCG instillations.

Heatmap of innate immunity genes grouped by gene clustering and average linkage (**A**) and UMAP dimensional analysis (**B**) show distinct gene expression and clustering of BBN exposed bladders compared to controls with the most marked activation among BBN samples following BCG therapy. Associated volcano plots highlight individually differentiated genes by log fold-change and significance activated by BBN carcinogen (**C, D, E**). Radiotherapy did not activate any genes in the NanoString Innate Immunity panel (**F**) compared to robust activation of innate immune genes following BCG instillations (**G, H**).

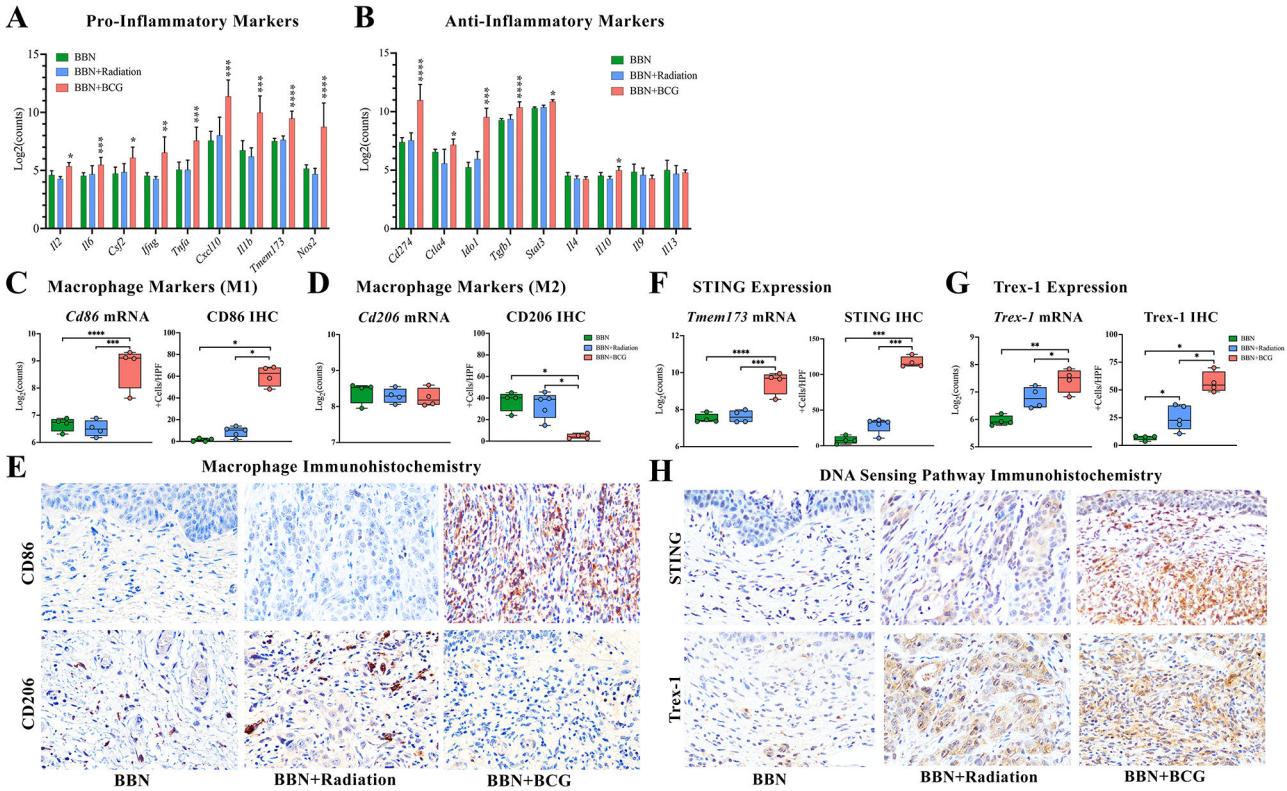

Figure 4. BCG induced immunostimulatory response is consistent with STING expression.

BCG induced expression of (**A**) typical pro-inflammatory markers and (**B**) certain anti-inflammatory markers along with (**C, E**) increased immunostimulatory macrophage marker *Cd86*. (**D, E**) RT induced protein expression of immunosuppressive macrophage marker CD206, despite no significant change in mRNA levels of *Cd206*. (**F, H**) STING is significantly elevated following BCG instillations at both mRNA and protein levels but was unchanged following radiotherapy. (**G, H**) BCG elevated levels of *Trex1* by both mRNA and protein expression while radiotherapy induced only protein expression of Trex-1. ***** $p < 0.05$, ******$p < 0.01$, *******$p < 0.005$, ********$p < 0.001$. Images at 40x magnification.

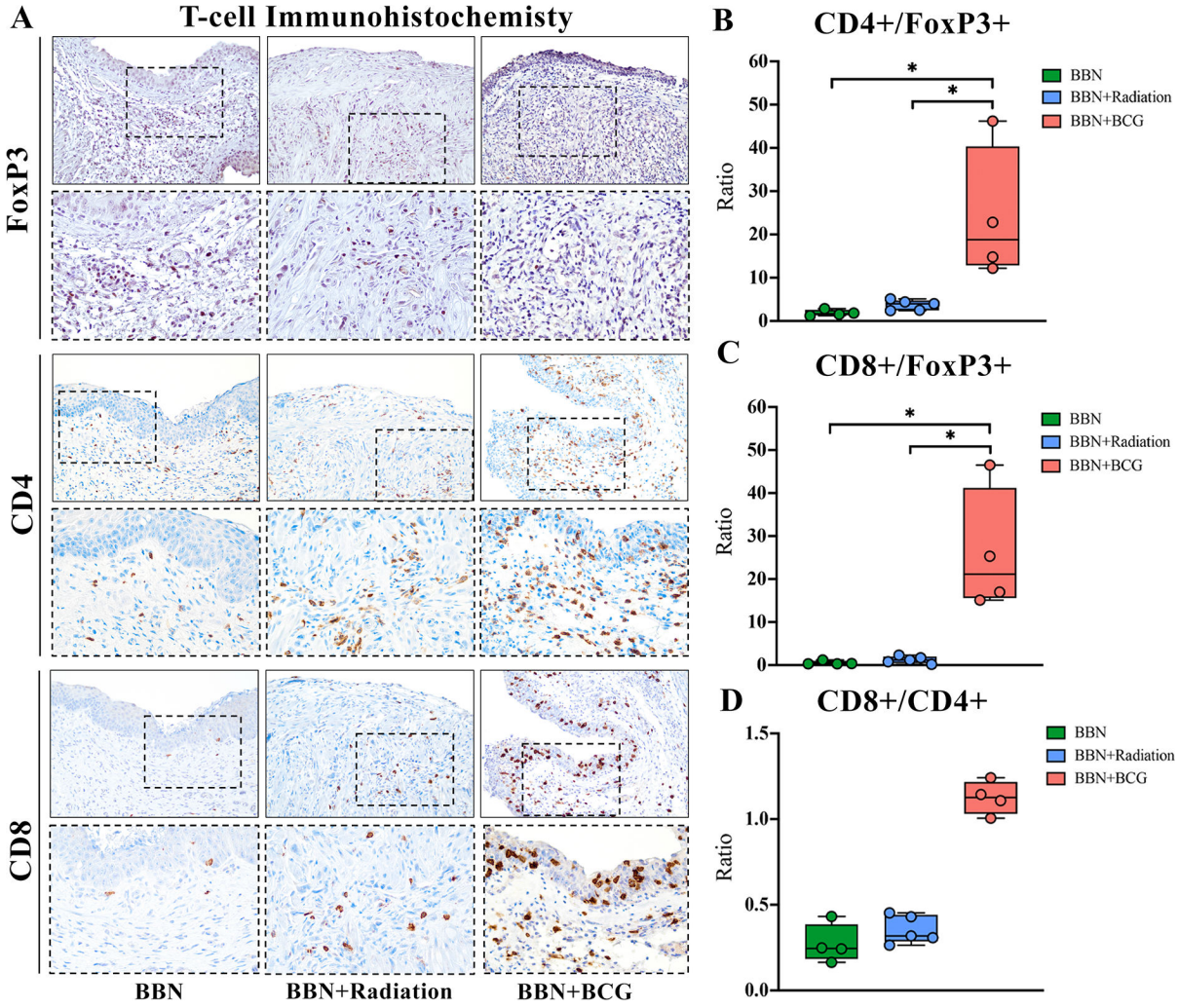

Figure 5. BCG instillations induced greater recruitment of T-effector cells to the bladder microenvironment compared to radiotherapy.

(A) Immunohistochemistry for Treg marker FoxP3, and Teff markers CD4 and CD8 show increased infiltration of Teff cells following BCG instillations as well as (**B, C**) increased Teff/Treg ratios. CD8+/CD4+ ratio shows a trend toward higher number of CD8+ T-cells. ***** $p < 0.05$. Solid border images 20x magnification, inset dashed border images 40x magnification.

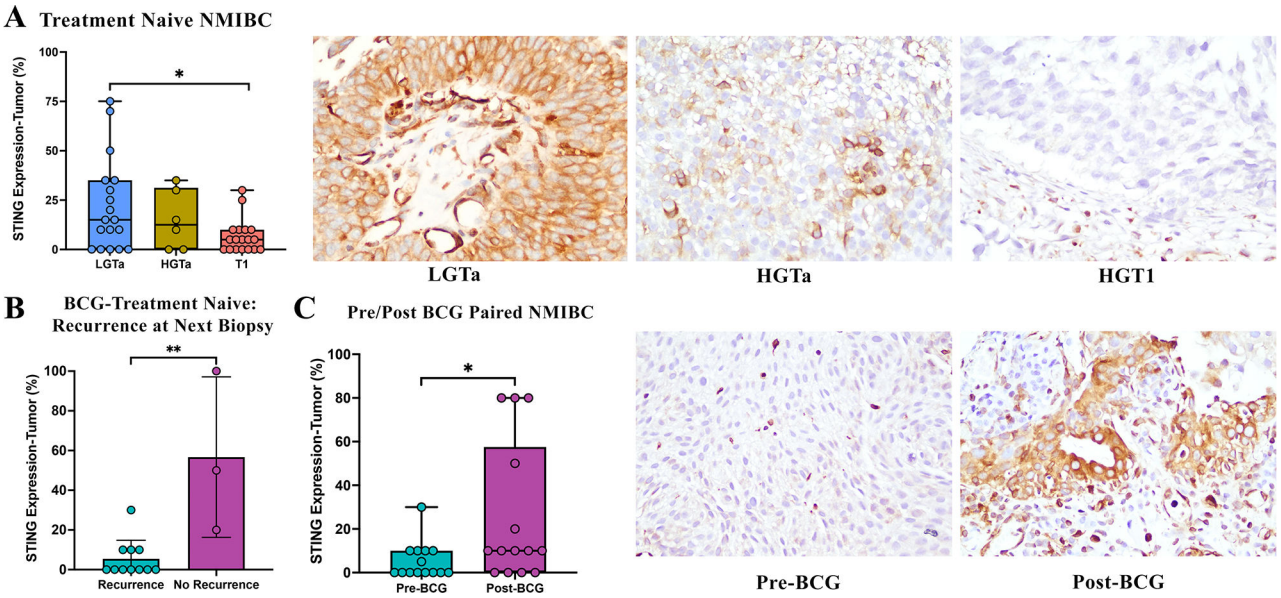

Figure 6. STING expression in human NMIBC.

(A) STING expression in tumor cells of treatment naïve samples decreases with progression of grade and stage. (B) Baseline expression of STING in pre-treated samples was higher in tumors of patients who had a positive response to BCG, with no tumor recurrence at their next biopsy following full BCG induction therapy. (C) Patients with tumor recurrence following BCG had higher STING protein expression in recurrent tumor samples post-BCG therapy.